Effects of separately laser-induced metal vapor amounts on the stability of a TIG arc

Insa Henze[a,*], Thorsten Mattulat[a], Peer Woizeschke[a]

[a]BIAS - Bremer Institut für angewandte Strahltechnik GmbH, Klagenfurter Straße 5, 28359 Bremen, Germany

Abstract

Arc stability during welding can be improved by using a laser process and the associated implementation of a hybrid welding process. Various effects are assumed to be the causes of the process stabilization by the additional laser beam. To investigate the metal vapor influence in a more decoupled manner, the metal vapor in this study is generated by a laser beam guided on an external substrate. The laser beam axis is oriented horizontally and thus perpendicular to the simultaneously ignited arc between a TIG welding torch and a counter electrode. The amount of metal vapor is adjusted by varying the laser power. The laser process causes the arc voltage to increase with the amount of metal vapor. This implies an increasing electrical resistance, which affects arc stability.

Keywords: laser welding; arc welding; metal vapor; arc stability

1. Introduction

Combining an arc welding process with a laser beam process can increase the arc stability due to synergetic effects and thereby improve the welding process. For example, Cui et al., 1992, showed an influence of the laser process onto the current density distribution in arc welding, which resulted in a reduced current channel cross-section and a more concentrated arc and, therefore, a deeper melting pool. Experiments on steel substrates carried out by Kling et al., 2007, furthermore showed the potential for guiding the arc using the laser beam. The alignment of the arc towards the laser beam already occurs at low laser powers and enables the increase of welding velocities by up to 60%.

---

* Corresponding author. Tel.: +49-421-218-58136; fax: +49-421-218-58063
E-mail address: henze@bias.de.

There are currently numerous approaches in the literature explaining the dominant causes of arc stabilization. Among others, the increased temperature, Schnick et al., 2009, and laser-induced metal vapor, Cui et al., 1992, are often mentioned as reasons for an increased conductivity in the arc, and therefore the stabilization of the arc by the laser beam. Metal vapor is generated during the laser welding process when the material temperature exceeds the vaporization temperature, especially in laser deep penetration welding. Here, the intensity of the laser beam at the material surface exceeds a material-specific critical value, and the formation of a vapor capillary, also known as a keyhole, takes place, Lee et al., 2002. The formation of this keyhole increases the absorption of the laser beam due to multiple reflections, Lee et al., 2002, and thereby, for example, increases the penetration depth in comparison to heat conduction welding, Stritt et al. 2010. The formation of a highly dynamic keyhole also increases the amount of metal vapor. The high recoil pressure and process dynamics in the keyhole result in an accelerated ejection of metal vapor out of the keyhole during the laser welding process, Lee et al. 2002.

A separate consideration of the individual effects of the laser process on arc stability to determine the dominant effects is challenging. Regarding the influence of laser-induced metal vapor, various explanations have been made. Cui et al., 1992, assumed a reduction of the resistance in the arc column due to the laser-induced metal vapor plasma, meaning that the most favorable contact point for the arc base is located in the area of the metal vapor plasma. Schnick et al., 2009, assumed an increase of the resistance in the arc and, therefore, also an increase of the arc voltage, especially with high amounts of laser-induced metal vapor, which cools the arc temperature because of its significantly lower temperature. This correlates with the findings of simulative studies reviewed in Murphy, 2010, on the influence of metal vapor in arc welding. It is assumed that the two effects are conflicting. On the one hand, there is an increase in conductivity due to the increase in electrical conductivity because of small quantities of metal vapor at low temperatures resulting from the lower ionization energy of the metal atoms. The generated metal vapor at the anode flows into the arc and is ionized more easily during the arc welding process, which is visible by measuring the arc spectrum, Tanaka et al., 2020. On the other hand, there could be a reduction in temperatures at high quantities of metal vapor due to the higher radiation emission of the metal vapor compared to argon, Murphy, 2010. It is assumed from the simulations that the lower arc temperature results in a decreased arc conductivity and, hence, a decreased arc voltage. An increased arc voltage, and therefore conductivity, is assumed to be accompanied by a decreased arc stability, Cui et al., 1992.

To improve the understanding of arc welding processes and especially laser-arc hybrid welding processes, this study examines the influence of different metal vapor amounts on arc stability. The metal vapor is generated separately by a laser welding process on a separately laterally positioned substrate material. It is assumed that the metal vapor flows out of the keyhole in the direction of the arc due to the recoil pressure and interacts with the arc without preheating the electrodes of the arc welding process. This enables a separate comparison of the effects of metal vapor on arc stability without considering the effects of preheating. The metal vapor amount was varied by varying the laser power and the focal plane at a constant focal diameter and welding velocity.

2. Experimental

The basis of the experiments was a separate consideration of the influence of metal vapor on arc stability. The metal vapor was generated using a separate laser welding process. The arc axis was oriented vertically, and the laser beam axis was orientated horizontally; hence, they were arranged perpendicular to each other, as shown in Fig. 1. The arc was ignited before the laser beam to measure the arc properties without metal vapor
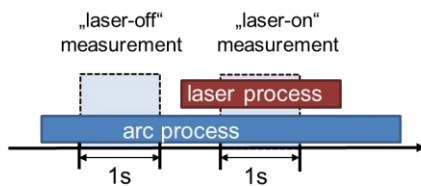
("laser-off" measurement).

The experiments were carried out using a TRUMPF TruDisk 12002 laser source in combination with an Abicor Binzel Abiplas MT 500 W TIG-welding torch and an EWM Tetrix 500 AC/DC Synergic welding power source. The welding power source was current regulated. The welding current was kept constant adjusting the welding voltage during the process. An optical fiber with a core diameter of 200 µm was used in combination with a one-to-one imaging ratio. The beam diameter on the substrate surface was adjusted by defocusing the laser beam focus (focal plane) out of the substrate. The aluminum alloy EN-AW-5083 with a thickness of 5 mm was used as substrate material; the chemical composition is shown in Table 1. The used process and shielding gas was a mixture of argon and helium (Ar 25 L/min, He 2.5 L/min). Fig. 2 displays the ionization energy and the emitted wavelengths of the elements in the process gas as well as the main elements in the substrate material.

The substrate material was moved to realize the process movement, whereas the arc and the laser beam were kept stationary. Tungsten electrodes WLa 15 (Ø 3.2 mm) were used for the welding torch and the water-cooled counter electrode. A ceramic sheet was positioned as a shielding plate in front of the counter electrode to avoid the heating of the electrode by reflected laser beam radiation from the laser welding substrate. Fig. 1 shows the experimental setup.

Table 1. Chemical composition of EN-AW 5083 (AMCO Metall-Service GmbH 2021)

Element	Si	Fe	Cu	Mn	Mg	Cr	Zn	Ti
Content [wt.-%]	0.4	0.4	0.1	0.4-1.0	4.0-4.9	0.025-0.25	0.25	0.15

Fig. 1. Experimental setup and measuring principle for the metal vapor amount (below) and arc stability measurements.

element	emitted wavelength [nm]
Ar I	763, 794, 811, 842
He I	706, 728
laser	1030 ± 10*
Al I	394, 396
Mg I	382, 470, 518
Mg II	821, 883
Mn I	470, 482, 551

Source: NIST Atomic Spektra Database; URL: https://physics.nist.gov/
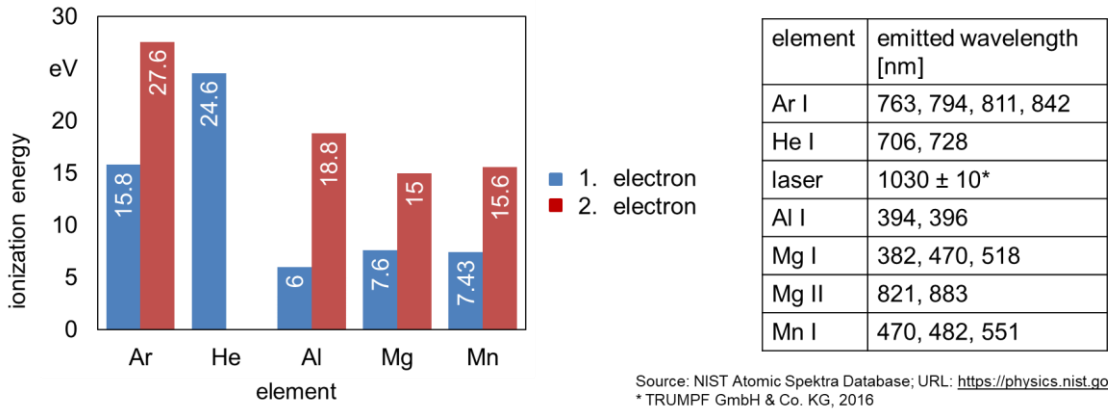* TRUMPF GmbH & Co. KG, 2016

Fig. 2. Ionization energy of the elements of the process gas and the substrate material

The metal vapor amount was varied by varying the laser power P_L and the welding velocity at a constant focal diameter. The laser spot diameters d_L of 370 µm and 520 µm on the workpiece surface were used. The laser power was adjusted in five steps depending on the averaged intensity. The averaged intensity $\overline{I_L}$ was calculated with equation (1):

$$\overline{I_L} = \frac{P_L}{A_L} = \frac{P_L}{\frac{\pi}{4}*d_L^2} \tag{1}$$

It is assumed that the metal vapor amount depends on the intensity and, therefore, the penetration depth. Separate experiments with a spot diameter of 370 µm on the workpiece surface were carried out as a preliminary test to investigate the correlation. Hereby, the same experimental setup was used as for the main experiments without the ignition of the arc (see Fig. 1). An aluminum sheet was positioned towards to the substrate material during the laser process, upon which the generated metal vapor and other process emissions condensed; this is hereafter referred to as the deposition sheet (see Fig. 1). The amount was evaluated optically and by measuring the weight difference of the deposition sheet with a fine balance before and after the laser process. Three samples were welded for every parameter set.

To assess the flow properties of the metal vapor, schlieren photographs were made with a Vision Research Phantom VEO 410 L high-speed camera for several parameter sets of the combined process. These also enabled an additional qualitative visualisation of the metal vapor amount.

The arc stability was evaluated by measuring the arc voltage with a RIGOL DS 1000 digital oscilloscope with a measuring frequency of 25 kHz. For each sample, the averaged arc voltage was calculated over a duration of 1 s for both the "laser-off" and "laser-on" periods. The arc spectra were detected by a Stellar Net. Inc Silver Nova spectrometer. Four samples were welded for every parameter set. For each parameter set, the four recorded spectra were averaged. The material was cleaned with ethanol prior to the experiments and the electrodes were abraded before each parameter set. Table 2 summarizes the constant welding parameters. Table 3 shows the varied parameters.

Table 2. Welding and measuring parameters.

| Welding speed	1.0	m/min
Shielding gas	Ar: 25, He: 2.5	L/min
Arc current	10	A
Distance between electrodes	15	mm
Oscilloscope measuring frequency	25000	Hz
Spectrometer measuring frequency	20	Hz

Table 3. Variated welding parameters (the parameters in bold were used for the schlieren photographs)

| Spot diameter (substrate surface) in μm		Laser power in W				
370		400	**600**	**900**	1300	**1700**
520	562	790	1185	1778	2568	3358
Intensity in 10^6 W/cm^2	0.265	0.372	0.558	0.837	1.2091	1.5811

3. Results

The results of the measurement of the influence of the laser power on the metal vapor amount are shown in Fig. 3. The diagram shows the median value and the minimum and maximum measured values (range) of the weight difference of the deposition sheet, which increases with increasing laser power. The optical consideration shows an increasing area of condensed vapor on the sheet, whereby the color becomes darker with increasing laser power. The sheets also had an increasing number of adherent spatters, with the amount also increasing with laser power. Neither measurements showed metal vapor at the lowest laser power of 400 W.

deposition sheet:

| 400 W | 600 W | 900 W | 1300 W | 1700 W |
laser power
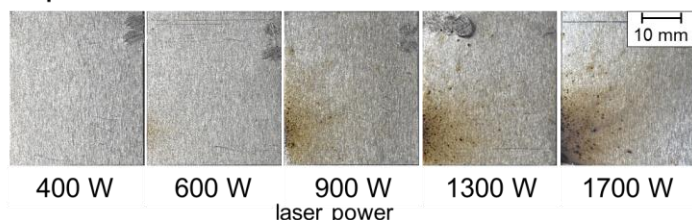
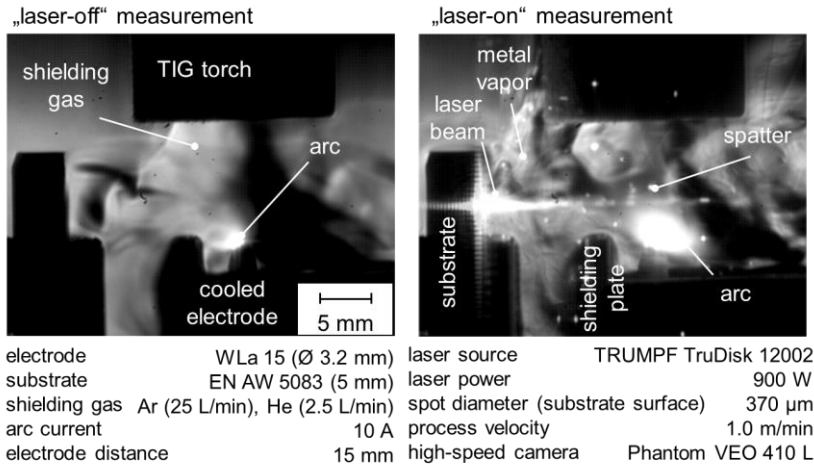| deposition sheet | EN AW 1050A (1.5 mm) |
substrate	EN AW 5083 (5 mm)
sheet distance	12 mm
laser source	TRUMPF TruDisk 12002
process velocity	1.0 m/min
spot diameter (substrate surface)	370 μm
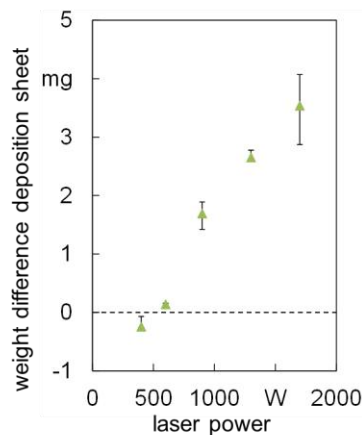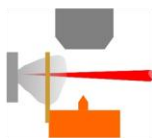
Henze 2021

BIAS ID 210188

Fig. 3. Influence of the laser power on the metal vapor amount on the deposition sheet

The schlieren photographs also implied an increasing vapor amount for higher laser powers as well as the generation of spatters in the welding process. The photographs showed that most of the generated metal vapor flowed in the direction of the arc. It expanded after the keyhole exits over a large area, and thus it was distributed over the complete length of the arc while part of it flowed out of the process zone at the top and bottom (see Fig. 4). An influence of the spatters on the arc was not detectable.


electrode	WLa 15 (Ø 3.2 mm)	laser source	TRUMPF TruDisk 12002
substrate	EN AW 5083 (5 mm)	laser power	900 W
shielding gas	Ar (25 L/min), He (2.5 L/min)	spot diameter (substrate surface)	370 µm
arc current	10 A	process velocity	1.0 m/min
electrode distance	15 mm	high-speed camera	Phantom VEO 410 L

Henze 2021   BIAS ID 210189

Fig. 4. Example for a schlieren photograph during the "laser-off" (left) and "laser-on" measurements at a laser power of 900 W.

Fig. 5 shows an example of a spectrogram of the emitted wavelength in the arc during the "laser-off" and "laser-on" measurements. The values are averaged for a measuring time of one second and across the four measurements. Furthermore, the diagram shows the emission transition probability of the elements contained in the used material with the highest wt.-%, of the used gases and the laser beam. During the "laser-off" measurement, the spectrogram showed high intensities for wavelengths near the highly probable Ar I wavelengths. The He I wavelengths were not detectable. It was similar for all tested "laser-off" parameters as well as for the "laser-on" measurement at a laser power of 400 W at a spot diameter of 370 µm and a laser power of 562 W at a spot diameter of 520 µm. In the remaining "laser-on" measurements, the measured wavelengths with high intensities were displaced to the highly probable Mg I and Al I wavelengths and those with lower intensity to the Mg II and Mn I wavelengths. The intensity of the Ar I wavelengths during the "laser-on" measurements with wavelengths of the metal vapor elements constantly decreased with increasing laser power. After the "laser-on" measurement, the arc spectrum returned to a shape comparable to the "laser-off" measurement.
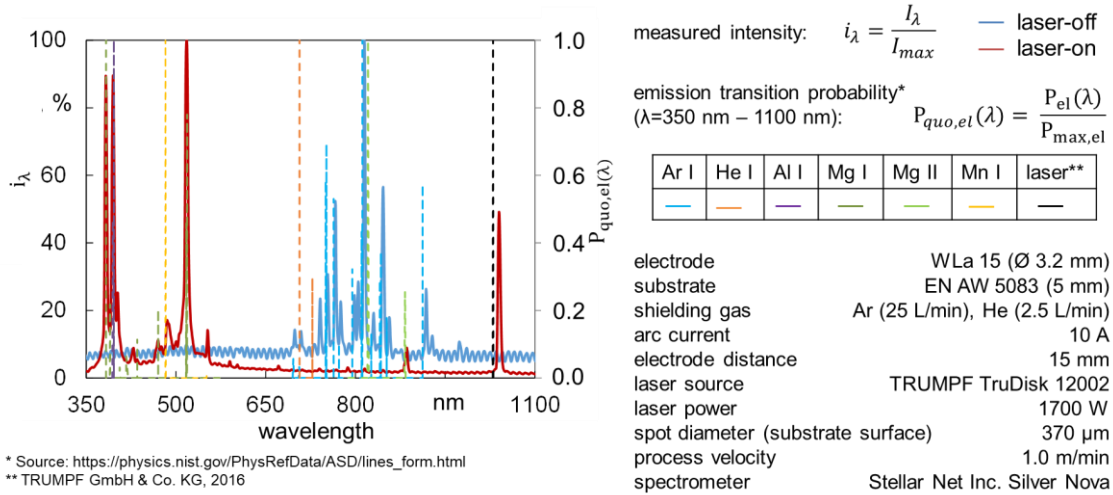
Fig. 5. Measurement of the arc spectrum with ("laser-off") and without laser-induced metal vapor; data source: National Institute of Standards and Technology, 2018 and TRUMPF GmbH & Co. KG, 2016.

The difference in the arc voltage depending on the averaged laser beam intensity is illustrated in Fig. 6. The diagram shows the median value across the four measurements and the range of the voltage difference. The measurement of the arc voltage during the "laser-on" periods showed an increasing arc voltage for all investigated parameters, except for the lowest investigated laser intensities. For both beam spot diameters on the workpiece, the voltage difference increases rapidly when exceeding a critical intensity. Above this critical threshold, however, it does not follow a clear trend. For the 370 µm spot diameter, the voltage difference decreases slightly with increasing beam intensity, while for the 520 µm spot diameter, the trend is rather increasing. After the "laser-on" measurement, the arc voltage returns to the previously measured voltage of the "laser-off" measurement.
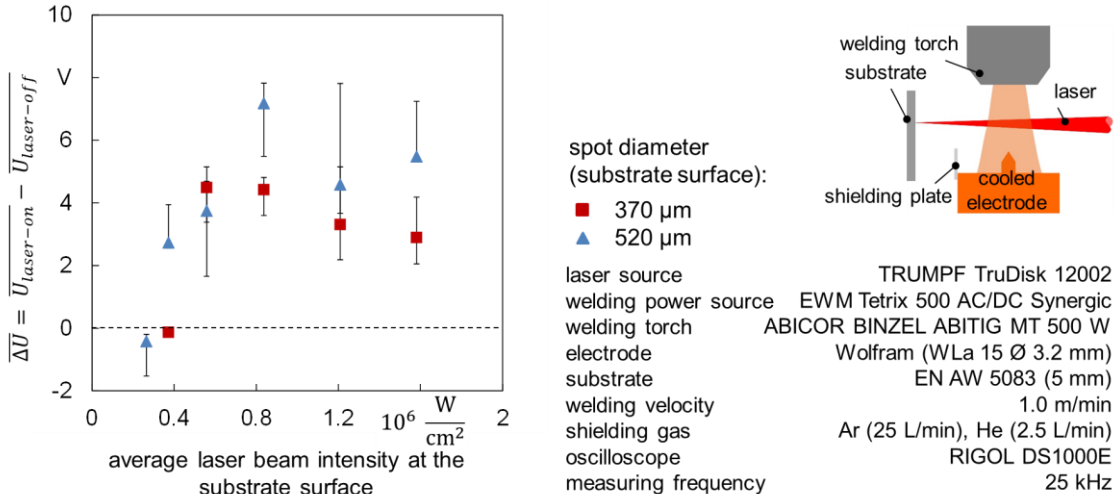
Fig. 6. Arc voltage difference for "laser-on" and "laser-off" periods in relation to the averaged laser beam intensity on the workpiece surface by varying the laser power and the spot diameter on the workpiece.

4. Discussion

The adjustability of the metal vapor amount was shown by separate experiments. The metal vapor amount increased with increasing laser power. At a laser power of 400 W, the metal vapor amount was too low to detect at the metal sheet. The spectrogram of the measurements during the laser-arc process confirmed these findings by detecting characteristic elements from the welded material inside of the arc only for laser powers above 400 W. In all samples with confirmed metal vapor generation from the deposition sheet, the wavelengths of the metal ions of Al, Mg and Mn, the main contents of the substrate material, were detected in the arc spectra.

The schlieren photographs confirmed the separated metal vapor deposition into the arc. As expected according to Lee et al., 2002, the metal vapor flowed out of the keyhole in the direction of the arc because of the high recoil pressure and process dynamics. The photographs also showed a high divergence of the metal vapor after exiting the keyhole, resulting in a vapor flow into the arc across the whole arc length.

All experiments showed that the measured arc properties were only changed during the "laser-on" measurement when metal vapor was generated. This enables a comparison of the arc properties with and without metal vapor and, therefore, the investigation of the influence of metal vapor on a TIG arc with separate laser-generated metal vapor.

The spectrogram showed that the metal vapor elements were ionized inside the arc as expected according to Tanaka et al., 2020. The high arc spectral intensities changed from the Ar I wavelengths to the Mg I, Mg II, Al I and Mn I wavelengths for all measurements with detected metal vapor generation. The Ar I spectral lines that were detectable with a high intensity during the "laser-off" measurement were only clearly measurable with low laser intensities during the "laser-on" measurement. This is related to the lower required ionization energy of the metal vapor atoms in comparison to the argon atoms, as shown in Fig. 2 with data from National Institute of Standards and Technology, 2018. The higher intensity of the Al and Mg wavelengths compared to the Mn wavelengths could result from their higher amount in the material. For Mg, the ionization energy of the second electron was the lowest of all elements in the arc. Therefore, the second electron was also emitted, and the Mg II wavelengths were detectable.

The measurement of the arc voltage showed an increased voltage at a constant arc current for all laser powers where metal vapor was generated. The metal vapor generation was confirmed in the spectrogram and the separate investigation of the metal vapor amount. The increased arc resistance, and therefore the decreased arc conductivity due to the metal vapor influence, corresponded with the results from the simulative studies on the influence of metal vapor in arc welding, Murphy, 2010. The decreased conductivity was assumed with decreased stability. The increased median values and range of the arc voltage at higher laser intensities, and therefore metal vapor amounts, indicated a decreased stability with increasing metal vapor amount. A decreased arc voltage, and therefore increased arc stability, was only measurable for samples where the spectrogram did not show any metal vapor in the arc. Therefore, the decreased voltage cannot be attributed to metal vapor but only to a self-stabilization of the arc at a constant arc current.

5. Conclusion

Based on the investigations, it can be concluded that
- the separate generation of metal vapor using an external laser process that flows into the welding arc due to recoil pressure enables an investigation of the influence of metal vapor on arc processes due to a direct comparison of the arc properties with and without metal vapor.

- the injection of metal vapor into the arc process without any side effects of the laser process on the arc (e.g. preheating) increases the arc voltage at a constant arc current, which means an increased arc resistance and, therefore, decreased arc conductivity and stability.
- the lower required ionization energy of the atoms in the metal vapor in comparison to the process gas results in a preferred ionization of the metal atoms, which is visible due to a shift of the emitted wavelengths in the arc spectrum.

Acknowledgements

References

AMCO Metall-Service GmbH (2021): Technisches Datenblatt EN AW-5083 (AlMg4.5Mn). Available online at https://amco-metall.de/fileadmin/downloads/Datenblaetter/Datenblatt__AMCO_5083.pdf, checked on 3/8/2021.

Cui, H.; Pursch, Heinz; Ruge, J.; Wendelstorf, Jens; Wohlfahrt, H. (1992): Laserinduziertes Fokussieren des WIG-Lichtbogens. In: DVS-Deutscher Verband für Schweißen und verwandte Verfahren (Hg.): DVS Berichte Band 146, pp. 139–143.

Kling, R.; Otte, F.; Stahlhut, Ch; Hermsdorf, J. (2007): Minimale Laserleistung mit Lasern angepasster Strahleigenschaften für das Laser/MSG-Hybrid-Schweissen in Fertigungssystemen für die Fahrzeugfertigung. In: DVS Verlag GmbH (Hg.): DVS Berichte Band 244, Bd. 244. With assistancs of Middeldorf K. Große Schweißtechnische Tagung 2007. Basel. DVS Deutscher Verband für Schweißen und verwandte Verfahren e.V., pp. 409-418.

Lee, Jae Y.; Ko, Sung H.; Farson, Dave F.; Yoo, Choong D. (2002): Mechanism of keyhole formation and stability in stationary laser welding. In: *J. Phys. D: Appl. Phys.* 35 (13), pp. 1570-1576. DOI: 10.1088/0022-3727/35/13/320.

Murphy, Anthony B. (2010): The effects of metal vapour in arc welding. In: *J. Phys. D: Appl. Phys.* 43 (43), p. 434001. DOI: 10.1088/0022-3727/43/43/434001.

National Institute of Standards and Technology (2018): NIST: Atomic Spectra Database Lines Form. Available online at https://physics.nist.gov/PhysRefData/ASD/lines_form.html, updated on 11/6/2021, checked on 3/12/2021.

Schnick, M.; Rose, S.; Füssel, U.; Mahrle, A.; Demuth, C.; Beyer, E. (2009): Numerische und experimentelle Untersuchungen zur Wechselwirkung zwischen einem Plasmalichtbogen und einem Laserstrahl geringer Leistung. In: DVS Media GmbH (Hg.): DVS Berichte Band 258. Große Schweißtechnische Tagung. Düsseldorf. DVS-Deutscher Verband für Schweißen und verwandte Verfahren e.V., pp. 16-21.

Stritt, Peter; Weber, Rudolf; Graf, Thomas; Müller, Steffen; Ebert, Christian (2010): Laser power modulation at the threshold from heat-conduction to deep-penetration welding. In: International Congress on Applications of Lasers & Electro-Optics. ICALEO® 2010: 29th International Congress on Laser Materials Processing, Laser Microprocessing and Nanomanufacturing. Anaheim, California, USA, September 26–30, 2010: Laser Institute of America, pp. 217–224.

Tanaka, Keigo; Shigeta, Masaya; Tanaka, Manabu; Murphy, Anthony B. (2020): Investigation of transient metal vapour transport processes in helium arc welding by imaging spectroscopy. In: *J. Phys. D: Appl. Phys.* 53 (42), p. 425202. DOI: 10.1088/1361-6463/ab9ce4.

TRUMPF GmbH & Co. KG (2016): TRUMPF TruDisk 12002-Technisches Datenblatt.